DOI: 10.1002/ejic.201100254

Synthesis, Structure, and Magnetic Properties of $Cu_2L_2Cl_2$ (LH = *N*-Salicylidene-1,2-ethanediamine) – A New *S* = 1/2 Spin–Liquid Candidate

Olivo Piovesana,*[a] Brunetto Chiari,[a] Antonio Cinti,[a] and André Sulpice[b]

Keywords: Copper / Spin–liquids / Magnetic properties

The synthesis, room temperature crystal and molecular structure, and magnetic properties are reported for the new compound $Cu_2L_2Cl_2$, where L^- is the tridentate anion of *N*-salicylidene-1,2-ethanediamine. The compound crystallizes in the monoclinic space group $P2_{1/c}$ with a = 6.213(5) Å, b = 11.622(5) Å, c = 14.260(5) Å, β = 100.240(5)°, and Z = 2. The crystal consists of dichloro-bridged binuclear molecules. The four-membered Cu_2Cl_2 bridging unit is strictly planar owing to crystallographic inversion symmetry. The geometry at the copper(II) centers is approximately square pyramidal, with the base plane formed by the *cis*-nitrogen atoms and the phenolic oxygen atom of the tridentate L^- ligand and one chloride ion; the fifth, apical site is occupied by the basal chloride ligand of the neighboring copper center. The intradimer copper–copper separation is 3.271(1) Å. The out-of-plane Cu–Cl distance is 2.824(1) Å and the bridging Cu–Cl–Cu angle is 78.58(2)°. Unit a translations of the binuclear molecules generate ladder-like chains of copper atoms parallel to [1 0 0]. Each dimer is connected to each of its two nearest neighbors by Cu–Cl···H–N–Cu and Cu–O···H–N–Cu H bonding interactions. Interladder Cu–N–C–H···Cl–Cu and Cu–N–C–H···O–Cu interactions give rise to a 3D, coupled two-chain lattice. The dependence of the magnetization (M) on the applied magnetic field (H) up to 7.5 T at 1.7 K, and the temperature dependence of the inverse magnetic susceptibility (χ^{-1}) between 1.7 K and 250 K show that the compound behaves as an ideal S = 1/2 paramagnet. This persisting spin disorder is tentatively attributed to the formation of an unusual spin–liquid state where ferromagnetic and antiferromagnetic exchange interactions between the Cu^{II} centers cancel.

Introduction

Owing to large zero-point energy and quantum fluctuations, only He remains liquid when cooled to T = 0 K under its saturated vapour pressure.[1] Pressures higher than 2500 kPa have to be applied in order to obtain solid He. The interface between liquid and solid helium is also unique in being the only liquid–solid interface existing over a wide continuous temperature range (at constant pressure).[2]

Interestingly, condensed matter offers several examples of exchange-coupled magnetic systems that mimic liquid He behavior, which are commonly referred to as spin–liquids.[3,4]

Theoretically conceived by Anderson,[5] the spins in a "perfect" spin–liquid, even if strongly correlated, should remain disordered even at T = 0 K. This is because of the presence of an infinite number of different zero-energy spin configurations among which the system can fluctuate without any energy cost.[6–7] The search for materials that exhibit ideal spin–liquid physics has occupied experimentalists for decades with mixed results.[7–9]

Indeed, in real systems, a variety of perturbations (single-ion anisotropies, long range interactions, crystallographic disorder, application of pressure and/or magnetic fields, etc.) can relieve the degeneracy of the spin–liquid ground state and induce long range magnetic ordering.[10,11] Such crystallization typically occurs at very low temperatures (much smaller than predicted from the spin–spin interaction strength, as indicated by the Curie–Weiss temperature, θ_{CW})[8,11] with long range order coexisting with the spin–liquid phase.[12–13]The nature of the ordered phase and how it can coexist with spin–liquid-like behavior remain open questions.[14–15]

So far, most experimental strategies developed to obtain spin–liquid model systems have been based on frustrated magnetism. In a general manner, a spin system is said to be frustrated when it is not possible to find a configuration of spins to fully satisfy the interaction between every pair of spins, which induces a large degeneracy of ground states. This property can be caused, for example, by a competition between different kinds of interactions (e.g. Villain model,[16] Shastry–Sutherland model)[17] or, more commonly, by the geometry of the lattice, a situation known as geometrical spin frustration (GSF).[18] The simplest model of GSF is an isolated equilateral triangle of three identical, collinear (i.e. up and down) spins with uniform antiferromagnetic (AF) coupling between any two spin sites.[19] The

[a] Dipartimento di Chimica, Università di Perugia, Via Elce di Sotto 8, 06100 Perugia, Italy
[b] André Sulpice, Institut NEEL, CNRS & Université Joseph Fourier, 25 Avenue des Martyrs, BP 166, 38042 Grenoble Cedex 9, France

(twofold degenerate) ground state of a configuration where two given spins are antiparallel is a pair of singlet (S = 0) and a frustrated free spin. The three different possible pairings in the triangle give rise to a total of six different degenerate spin configurations. Owing to the system fluctuations between them, the three pairwise singlet states cannot be formed simultaneously. In three dimensions, a similar situation occurs for a regular tetrahedral plaquette.[19]

In light of these considerations it is not surprising that many reported AF spin–liquid lattices are based on triangular (or tetrahedral) building blocks.[3]

Most spin–liquid candidates studied so far have been ionic compounds where the ligands bridging the magnetic centers are simple anions, such as O^{2-}, F^-, etc., and the lattice symmetry is, in general, relatively high.

Much less attention has been devoted to molecular-based spin–liquids.[20] Although, in comparison with ionic compounds, molecular compounds potentially offer a much wider variety of electronic structures and crystal lattices, they are more difficult to study. In molecular crystals the constituent magnetic molecules are most often connected by Cu–Cl···H–C–N–Cu, Cu–N–H···H–C–N–Cu, or C–H···H–C pathways with no particularly short H···Cl and H···H distances. The issue of whether these interactions are H bonds with electrostatic and polarization contributions or mere space-filling van der Waals interactions (a matter which clearly involves their possible magnetic role) has been the subject of intense debate for about two decades.[21–24] Owing to this, reliable experimental results for spin–liquid states in molecular systems require the use of demanding techniques,[7] which are often difficult to apply. As an example, single crystal inelastic neutron scattering (SCINS) experiments can provide crucial information on the nature of spin correlations and excitations but need very large deuterated crystals that can rarely be obtained in molecular chemistry.

Here we report the structural and magnetic properties of the new molecular compound $Cu_2L_2Cl_2$ (L^- = tridentate anion of *N*-salicylidene-1,2-ethanediamine). The compound has an unexpected magnetic response as it behaves as a pure spin S = 1/2 paramagnet in spite of a chemically ordered structure formed by bis(μ-chloro)-bridged dimeric units with an intradimer Cu···Cu separation of 3.271(1) Å. This anomalous magnetic behavior is tentatively attributed to the formation of a new spin–liquid state.

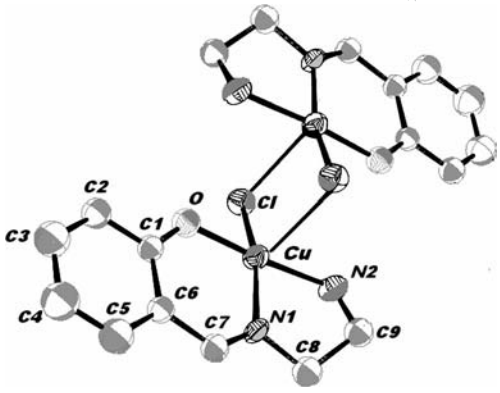

Figure 1. View of the molecular structure of the binuclear units in $Cu_2L_2Cl_2$. Hydrogen atoms have been omitted for clarity. Unlabeled atoms are related to labeled atoms by inversion symmetry.

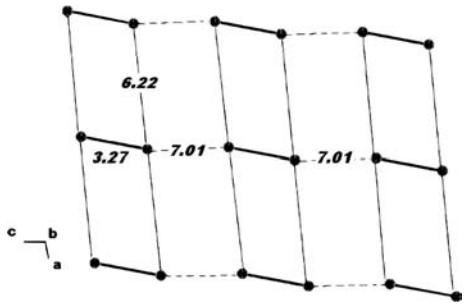

Figure 2. Schematic view of the three dimensional lattice formed by the [1 0 0] directed two-chain ladders in $Cu_2L_2Cl_2$. Numbers indicate Cu···Cu distances given in Å units.

Table 1. Crystallographic data for $Cu_2L_2Cl_2$.

Empirical formula	$Cu_2(C_9H_{11}N_2O)_2Cl_2$
Crystal class	monoclinic
Space group	$P2_1/c$
a	6.213(5) Å
b	11.622(5) Å
c	14.260(5) Å
β	100.240(5)°
V	1013.3(10) Å^3
Z	2
F(000)	532
Fw	524.56
T	20 °C
Radiation	Mo-K_α
λ	0.71069 Å
ρ	1.719 g/cm^3
μ	2.384 mm^{-1}
R (gt)	0.0403
wR (gt)	0.0726

Results

Description of the Structure

Structural information for $Cu_2L_2Cl_2$ is reported in Figures 1, 2, Tables 1, 2, 3, and 4. The crystal consists of dichloro-bridged binuclear molecules.

The four-membered Cu_2Cl_2 bridging unit is strictly planar owing to the presence of crystallographic inversion symmetry. The geometry at the Cu^{II} centers is approximately [4 + 1] square pyramidal, with the base plane formed by the *cis*-nitrogen atoms and the phenolic oxygen atom of the tridentate L^- ligand and one chloride ion; the fifth, apical site is occupied by the chloride ligand that is in the base plane of the other copper center in the dimer. The intradimer copper–copper distance is 3.271(1) Å. The bond lengths and angles in the basal plane are comparable with corresponding values reported in a number of other structurally related copper(II) complexes.[25–28] The out-of-plane Cu–Cl distance of 2.824(1) Å is in the range (2.70–3.37 Å) so far reported for similarly bridged copper(II) dimers, but

Table 2. Fractional atomic coordinates for $Cu_2L_2Cl_2$.

	x/*a*	*y*/*b*	*z*/*c*
Cu	–0.03174(6)	0.01695(3)	0.61060(3)
Cl	–0.15431(11)	–0.14441(4)	0.52353(5)
O	0.24720(7)	–0.05095(5)	0.65508(5)
N1	–0.00206(11)	0.12686(5)	0.71416(4)
N2	–0.30079(10)	0.10694(5)	0.55682(6)
C1	0.38373(9)	–0.02555(7)	0.73394(6)
C2	0.58311(12)	–0.08703(10)	0.75486(9)
C3	0.72933(15)	–0.06723(13)	0.83750(10)
C4	0.69160(18)	0.01474(13)	0.90275(9)
C5	0.49842(17)	0.07751(11)	0.88329(6)
C6	0.34306(13)	0.05902(8)	0.80024(5)
C7	0.15074(13)	0.13085(7)	0.78616(4)
C8	–0.19068(14)	0.20521(7)	0.70603(7)
C9	–0.27853(15)	0.22232(6)	0.60237(8)

Table 3. Bond lengths [Å] and angles [°] for $Cu_2L_2Cl_2$.

Bond lenths			
Cu–Cl	2.303(1)	C1–C6	1.417(2)
Cu–N2	2.005(1)	C2–C3	1.373(2)
Cu–N1	1.936(1)	C3–C4	1.381(3)
Cu–O	1.907(1)	C4–C5	1.390(2)
C8–N1	1.472(2)	C9–C8	1.495(2)
C7–N1	1.269(1)	C6–C7	1.442(2)
C9–N2	1.486(2)	C2–C1	1.415(2)
C1–O	1.316(1)	C6–C5	1.405(2)
Cu–Cu[a]	3.271(1)	Cu–Cl[a]	2.824(1)
Bond angles			
N2–Cu–N1	84.69(3)	C1–C6–C5	119.41(17)
N2–Cu–O	171.67(4)	C1–C6–C7	123.38(8)
N2–Cu–Cl	92.59(3)	C5–C6–C7	117.19(8)
N1–Cu–O	93.53(4)	C4–C5–C6	12.84(10)
N1–Cu–Cl	157.82(3)	C6–C7–N1	125.00(8)
O–Cu–Cl	92.08(3)	C9–C8–N1	107.80(7)
C3–C2–C1	121.13(10)	C9–N2–Cu1	107.28(5)
C2–C3–C4	121.89(13)	C7–N1–C8	120.76(8)
C2–C1–C6	117.56(8)	C7–N1–Cu	126.66(5)
C2–C1–O	118.29(8)	C1–O–Cu	126.93(5)
C6–C1–O	124.14(8)	C8–N1–Cu	112.42(5)
C3–C4–C5	118.15(12)	Cu–Cl[a]–Cu[a]	78.58(2)
C8–C9–C2	107.54(8)		

[a] = $-x$, $-y$, $-z + 1$.

Table 4. Possible hydrogen bonding in $Cu_2L_2Cl_2$.

Interdimer–intraladder				
	H···A	D–H···A	D···A	Cu···Cu
Cu[b]–N2[b]–H10[b,d]···O–Cu	2.885	167.6	3.823(2)	6.213(1)
Cu[b]–N2[b]–H10[b,d]···Cl[a]–Cu[a]	2.843	118.2	3.404(3)	6.118(1)
Interladder				
	H···A	D–H···A	D···A	Cu···Cu
Cu[c]–N1[c]–C7[c]–H5[c]···Cl–Cu	2.811	171.7	3.764(1)	7.012(1)
Cu[c]–N1[c]–C8[c]–H6[c]···O–Cu	2.667	146.9	3.511(1)	7.012(1)
Cu[c]–N1[c]–C7[c]–H5[c]···Cl–Cu[a]	2.811	171.7	3.764(1)	8.954(1)

[a] = $-x$, $-y$, $-z + 1$. [b] = $x + 1$, y, z. [c] = $-x$, y–1/2, $-z + 1/2 + 1$. [d] Bifurcated.

the bridging Cu–Cl–Cu angle of 78.58(2)° is smaller than that found in any other tetragonal pyramidal dichloro-bridged copper(II) dimer.[25–29]

Owing to the $P2_{1/c}$ crystal symmetry, the dimers have two different orientations in the crystal, which, if defined by the directions of the intradimer Cu···Cu bonds, form an angle of 13.9°. Unit *a* translations of the binuclear molecules with the same orientation generate two-legged ladders of copper atoms parallel to [1 0 0]. The copper atoms of adjacent rungs within each ladder interact through traditional Cu–Cl···H–N–Cu and Cu–O···H–N–Cu H bonding interactions.

Interladder interactions occur through less conventional Cu–N–C–H···Cl–Cu and Cu–N–C–H···O–Cu H bonding pathways (see Table 4), giving rise to the coupled two-chain lattice shown in Figure 2. The shortest interladder Cu···Cu separation is 7.012(5) Å.

Magnetic Properties

Figure 3 shows the dependence of the magnetization of the compound (*M*, per mol of Cu atoms) on the applied magnetic field (*H*) up to 7.5 T, at 1.7 K.

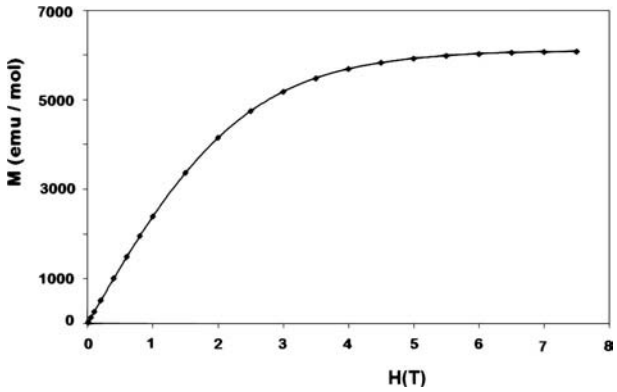

Figure 3. Dependence of the $Cu_2L_2Cl_2$ magnetization (*M*, per mol of Cu atoms) on the applied magnetic field (*H*) at 1.7 K. The best fit solid curve through the data points was obtained as explained in the text.

Data analysis was performed with the Brillouin law. For an ideal paramagnet of arbitrary spin-quantum number *S*, the magnetization is given in Equation (1).

$$M = N\, g\, \mu_B\, S\, B_S(X) \quad (1)$$

N is the Avogadro number, *g* the Lande *g* factor, μ_B the Bohr magneton, and $B_S(X)$ the Brillouin function for $X = (g\, \mu_B\, S\, H/k_B T)$, where k_B is the Boltzmann constant and *T* the temperature.[30]

The solid curve in Figure 3, which is in excellent agreement with the experiment, was obtained with $g = 2.14$ and $S = 0.51$. These values are typical for a (d^9) copper(II) single ion in a square pyramidal environment.[30]

In agreement with the magnetization results, the temperature dependence of the inverse magnetic susceptibility (χ^{-1} per copper) between 1.7 K and 250 K shows that the

compound behaves as an ideal Curie paramagnet. Indeed, the experimental data are quite well reproduced by the Curie law, see Equation (2).

$$\chi^{-1} = 3\ k_B\ T/[N\ g^2\ \mu_B^2\ S\ (S + 1)] \quad (2)$$

with $g = 2.14$ and $S = 1/2$. The experimental and theoretical χ^{-1} (T) dependence in the low temperature region are shown in Figure 4, where it can be seen that the Curie–Weiss temperature θ_{CW} is not significanty different from 0 K. The susceptibility is virtually field independent for $H \leq 1$ T.

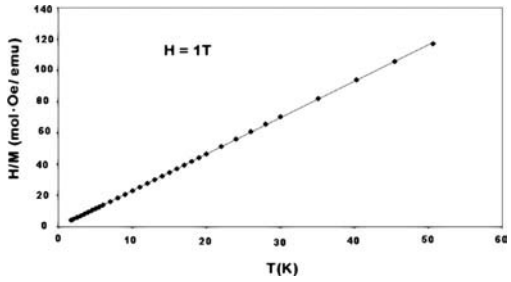

Figure 4. Temperature dependence of the inverse magnetic susceptibility (χ^{-1} per mol of copper atoms) for $Cu_2L_2Cl_2$.

No anomalies or history dependence are observed in the susceptibility at low temperatures indicating the absence of a transition to a long range ordered or a spin–glass-like state above 1.7 K.

Discussion

The magnetic results for $Cu_2L_2Cl_2$ are intriguing as they show that, in spite of a chemically ordered dimeric structure, the $S = 1/2$ spins remain fully disordered down to 1.7 K, a situation which, as suggested by the zero value of the Weiss constant, might persist to 0 K.

In principle, this behavior may be reconciled with three different situations, corresponding to magnetic lattices where: i) the Cu^{II} ions are magnetically diluted, ii) exchange coupled Cu^{II} dimers with degenerate $S = 0$ and $S = 1$ ground states do not interact between them, and iii) there are multiple ferromagnetic (F) and AF spin–spin interactions in the 3D structure that cancel each other out forming a highly degenerate spin–liquid state. We will now try to convince the reader that the third option is the most likely.

The magnetic and structural properties of Cu^{II} compounds built from bis(μ-chloro)-bridged binuclear units with parallel–planar geometry have been studied for over thirty years.[25–29]

As exchange coupling in Cu^{II} systems is largely isotropic,[30] the magnetism of a bimetallic cluster is well described by the Heisenberg Hamiltonian given in Equation (3), where J denotes the exchange coupling parameter and S_1 and S_2 are quantum–spin operators. Negative J refers to AF coupling (singlet ground state) and positive J refers to F interactions (spin–triplet ground state). The energy separation between the singlet and triplet states is $E_{ST} = E(\text{singlet}) - E(\text{triplet}) = 2J$ and can be evaluated by fitting the appropriate expression[30] for magnetic susceptibility to experimental data.

$$H = -2J\ S_1 \cdot S_2 \quad (3)$$

As first pointed out by Hatfield et al.,[28,29] the members of the parallel–planar family consisting of effectively isolated dimers exhibit a simple relationship between the E_{ST} values thus determined (which are always rather small and can also be equal to zero) and the quotient Φ/R, where Φ is the Cu–Cl–Cu bridging angle and R is the long out-of-plane Cu–Cl bond length in the Cu_2Cl_2 bridging unit. As described in detail elsewhere,[28,29] E_{ST} increases with increased Φ/R until it reaches a maximum value after which further increase in Φ/R leads to a reduction in E_{ST}. In the absence of an analytical expression, an intuitive, qualitative insight into the E_{ST} (Φ/R) dependence is offered by magnetic exchange theoretical models,[31–34] which interpret the J coupling constant for a weakly interacting spin pair in terms of competing F $(J_F > 0)$ and AF $(J_{AF} < 0)$ contributions, i.e. $J = J_F + J_{AF}$. This concept,[33] although qualitative in nature, is valuable in simply explaining the experimental sign of J in terms of the relative magnitude of J_F and $|J_{AF}|$, in predicting a zero value of E_{ST} for some Φ/R values where these two terms approximately cancel; a situation experimentally observed for $[Cu(Et_3en)Cl_2]_2$, where $\Phi/R = 35$ deg/Å[35] and, more importantly for this work, in enlightening the different physical significance (not revealed by magnetic susceptibility experiments) of the presence of doublet state magnetism in a bridged Cu^{II} dimer with $E_{ST} = 0$ and in a system of two noninteracting copper ions.[28,35,36a] In the former case the singlet and triplet states are energetically degenerate but the two copper ions can be strongly exchange coupled because J_F and J_{AF} are $\neq 0$. In the latter case there cannot be any correlation between the two copper ions as J_F and J_{AF}, which both involve two-center integrals,[33] are equal to zero, quite an unlikely circumstance for the bridged dimer with a short $Cu^{II}\cdots Cu^{II}$ separation seen in $Cu_2L_2Cl_2$.

Applying the empirical E_{ST} vs. Φ/R correlation to the $Cu_2L_2Cl_2$ dimeric unit, the observed Φ/R value of 28 deg/Å leads us to expect intradimer AF coupling with $E_{ST} \approx -20$ cm^{-1}.[28] Remembering that the hallmark of an intradimer AF interaction is the presence of a maximum in the χ vs. T plot (and hence a minimum in the $1/\chi$ vs. T plot) and that the temperature T_{max} for which the maximum (minimum) occurs is related to $2J$ through $|2J|/(kT_{max}) = 1.599$, (with $k = 0.695$ cm^{-1} K^{-1}),[36b] one should observe T_{max} at about 18 K, which is at variance with the experimental susceptibility data. In light of this, models describing $Cu_2L_2Cl_2$ as an assembly of either magnetically dilute Cu^{II} ions or isolated dimers with $E_{ST} = 0$ do not appear to be realistic.

This leads us to consider the possibility that the disordered spins in $Cu_2L_2Cl_2$ form a gapless spin–liquid where both nearest neighbor and H bond-mediated further

neighbor spin–spin correlations occur. If so, the system is described by a generalized Heisenberg model with not only the nearest neighbor interactions, see Equation (4).

$$H = -2\Sigma_{(i,j)}\, J_{ij}\, S_i \cdot S_j \quad (4)$$

Useful, albeit indirect, indications concerning the difficult problem of assessing the individual J_{ij} pathways are provided by the detailed structural and magnetic results obtained for another member of the parallel–planar Cu(μ-Cl)$_2$Cu family: Cu_2(1,4-diazacycloheptane)$_2Cl_4$ (CuHpCl), where, as summarized below, the combined effects of intradimer and H bond-mediated interdimer interactions have been reported to yield a frustration-induced 3D quantum spin–liquid.[38]

CuHpCl [monoclinic space group $P2_{1/C}$ with a = 13.406(3) Å, b = 11.454(2) Å, c = 12.605(3) Å, and β = 115.01(2)°][37] and $Cu_2L_2Cl_2$ are structurally related in that they are built from binuclear molecules where, as can be seen from Figures 1 and 5, the constituent copper atoms have similar tetragonal pyramidal [4 + 1] coordination geometry and are similarly bridged by two chloride anions in a basal to apical fashion. The intradimer Cu···Cu distance is 3.422(0) Å. As in $Cu_2L_2Cl_2$, the CuHpCl dimers stack up to form infinite two-legged ladders, this time along the [1 0 1] direction. Nearest neighbor copper atoms along the ladder legs are connected by conventional Cu–Cl···H–N–Cu H bonding interactions with a Cu···Cu separation of about 7.0 Å.

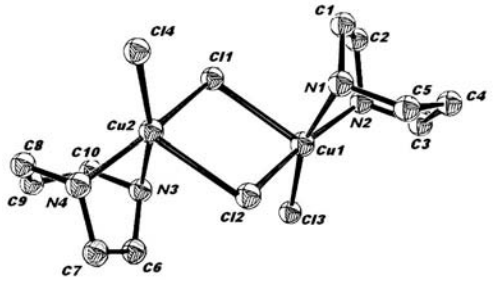

Figure 5. View of the molecular structure of the binuclear units in CuHpCl, hydrogen atoms have been omitted for clarity. The average intradimer Cu–Cu distance, the out of plane Cu–Cl distance, and the bridging Cu–Cl–Cu angle are 3.422(0) Å, 2.647(1) Å, and 86.9(0)°, respectively.

Less conventional Cu–Cl···H–C–N–Cu, Cu–N–H···H–C–N–Cu, or C–H···H–C interactions between ladders (the shortest Cu···Cu spacing is about 7 Å) give rise to a coupled two-chain lattice of copper atoms similar to that in $Cu_2L_2Cl_2$.[38]

Interestingly, the magnetic behavior of CuHpCl (which has been investigated extensively by magnetic susceptibility,[37,39–43] magnetization,[39–43] heat capacity,[40,41,44,45] NMR,[46–48] ESR,[42,43,49] and magnetic and thermal measurements under pressure)[50] is quite different from that of $Cu_2L_2Cl_2$. For example, magnetization data at low temperature show that CuHpCl is in a spin–0 singlet state below a H_{c1} critical field of 7.5 T, in a 3D ordered magnetic phase between H_{c1} and H_{c2} = 13 T, and in a fully polarized, gapped phase above H_{c2}.[39] Such diverse behavior observed in spite of the analogous binuclear units is clearly inconsistent with dominant intradimer exchange and suggests the presence of frustration effects. Indeed, a high sensitivity to changes, even small, in Hamiltonian (4) is characteristic of frustrated systems, as revealed, for example, by the quite different magnetic properties of isostructural Cs_2CuCl_4 and Cs_2CuBr_4.[51,52]

Perhaps most important is the fact that, so far, CuHpCl is the only compound structurally related to $Cu_2L_2Cl_2$ for which the network of significant magnetic interactions in Hamiltonian (4) has been explored by SCINS techniques.[38]

Although the complete spin Hamiltonian for CuHpCl remains to be solved and a detailed comparison between H bonding patterns in CuHpCl and $Cu_2L_2Cl_2$ cannot be made because the Hp ligand has two –N–H donors, whereas L^- has one –N–H donor and an $–O^-$ acceptor, SCINS data for CuHpCl help to answer the question of whether significant intermolecular spin–spin correlations occur in $Cu_2L_2Cl_2$, a prerequisite, together with the observed spin disorder, for a spin–liquid candidate. In particular, the neutron experiments for CuHpCl show that:

a) the intramolecular exchange, owing to frustration, provides a positive, F contribution to the energy of the ground state. As the latter is a gapped spin singlet with a negative total energy, its formation is allowed by the prevailing, combined negative, AF contributions from intermolecular, H bond-mediated exchange interactions. Of these, the data indicate that the most effective proceeds through a Cu–Cl···H–N–Cu pathway. As mentioned before, a similar pathway is present in the $Cu_2L_2Cl_2$ structure.

b) Table 4 and Figure 6 show that in the $Cu_2L_2Cl_2$ structure each of the two dichloro-bridged Cu(x, y, z) and Cu($–x$, $–y$, $–z$ + 1) dimer atoms (separated by ca. 3.27 Å) interact with the Cu^c($–x$, y – 1/2, $–z$ + 1/2 + 1) atom of a near neighbor molecule through Cu–N–C–H····Cl–Cu ex-

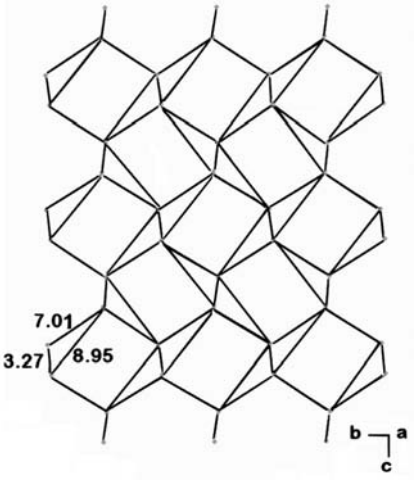

Figure 6. Lattice of interladder interactions mediated by the Cu–N–C–H···Cl–Cu hydrogen bonds in $Cu_2L_2Cl_2$. The view is perpendicular to the [1 0 0] direction. Similarly mediated Cu···Cu interactions in CuHpCl generate a topologically equivalent lattice of Cu atoms.

change pathways with Cu···Cu′′′ and Cu′···Cu′′′ separations of about 7 and 9 Å, respectively.

Closely similar triangles of interacting metal centers are found in the structure of CuHpCl where SCINS data indicate that the two intermolecular interactions are AF and principally responsible for the frustrated configuration of the intramolecular interaction.

Furthermore, in both $Cu_2L_2Cl_2$ (Figure 6) and CuHpCl (see part b of Figure 3 in ref.[38]), the connectivity of the magnetic sublattice formed by the three bonds is that of the geometrically frustrated Shastry–Sutherland model (a square lattice with alternating diagonal bonds on half the squares),[17] albeit with lower symmetry. The CuHpCl data show that this topology is important for promoting a spin–liquid state.

c) Even more relevant, the key message of the SCINS results is that the formation of the spin–liquid ground state in CuHpCl is the result of a delicate balance of energy terms of varying sign, a situation where tiny terms in Hamiltonian (4) can amplify their role to the point where they actually control the ground state.

To sum up, points a) and b) reinforce the view that neither the single Cu^{II} ions nor the $Cu_2L_2Cl_2$ dimers are magnetically isolated. Point c) leads us to suggest that the structural and/or chemical variations from CuHpCl to $Cu_2L_2Cl_2$ [which, as seen from the M(H) results, have quite significant magnetic consequences] induce a magnetic lattice where F and AF interactions cancel, giving rise to a 3D, macroscopically degenerate spin–liquid ground state.

This picture also explains the observed paramagnetism. The main energy scale for the fluctuatons of an anisotropic spin–liquid system is in the order[53] of $2S(\Sigma_d Z_d J_d) = 3\theta/(S + 1)$, where $\theta = 2(\Sigma_d Z_d J_d)\ S(S + 1)/3$ and is the Curie–Weiss temperature that depends on the sign and intensity of spin to spin interactions J_d, number of spins Z_d at distance d and spin quantum number S. Clearly, θ is zero if the summation of the $Z_d\ J_d$ terms pertaining to nearest and further neighbor spins is zero.

The proposed model is unprecedented and, clearly, further experiments on $Cu_2L_2Cl_2$ are required to confirm its spin–liquid nature. Work in this direction is interesting but challenging. The heart of the problem, which is general in the search for spin–liquids,[7–9,12] is that there is no single experimental feature that unambiguously identifies a spin–liquid state and, consequently, existing evidence for such states is circumstantial. The huge variety of unpredictable phenomena observed in recently characterized spin–liquid candidates further complicates the problem.

With this in mind, SCINS measurements, once suitable crystals are available, appear to be the most appropriate for future studies on $Cu_2L_2Cl_2$.

Experimental Section

Synthesis of $Cu_2L_2Cl_2$: $CuCl_2$ in methanol (20 mL, 0.50 M) was added dropwise to solution of 1,2-ethanediamine (60 mL, 0.17 M) in methanol at room temperature. A bluish suspension was formed, which was treated dropwise with water (10 mL). The suspension was then heated to 60 °C and treated dropwise with salicylaldehyde (25 mL, 0.40 M) in methanol. A dark green solution was obtained by heating the reaction mixture to reflux for about 10 min. The solution was filtered and allowed to stand at room temperature for 24 h. Bright, dark green crystals separated, which were collected by filtration and dried under vacuum; yield 1.15 g (44%); m.p. 248–250 °C. $C_{18}H_{22}Cl_2Cu_2N_4O_2$ (524.56): calcd. C 41.22, H 4.23, N 10.68; found C 41.10, H 4.32, N 10.60. Crystals suitable for X-ray analysis were obtained by recrystallization from methanol.

Magnetic Measurements

The microcrystalline powders used for the magnetic experiments were obtained by pulverizing samples of single crystals. Magnetization measurements up to 7.5 T at 1.7 K were performed with a commercial SQUID magnetometer (Metronique Ingeniérie). The powder was put in a very thin long Araldite container with magnetization negligible for any field and temperature of these experiments.

Variable temperature magnetic susceptibility measurements between 1.7 and 250 K were performed using both a Faraday-type magnetometer equipped with a continuous-flow cryostat built from Oxford Instruments and the SQUID magnetometer. Susceptibilities were corrected for the diamagnetism of the ligand system (-126×10^{-6} emu Oe^{-1} mol^{-1}/Cu). Our analyses used a temperature-independent paramagnetic term, $N\alpha$ of 60×10^{-6} emu Oe^{-1} mol^{-1}/Cu.

Crystallographic Data Collection and Structure Determination

A deep green prismatic crystal, with dimensions $0.15 \times 0.35 \times 0.20$ mm, was mounted on the goniometric head of an Xcalibur Single Crystal Diffractometer (model type CCD/PD). The diffractometer works with a four circle Kappa geometry. The cell parameters, listed in Table 1 together with additional crystal data, were determined using the full data collection. The data were corrected for Lorentz and polarization factors. The structure was solved by direct methods, with the SIR 97 program and refined by the full-least-square-matrix method with the SHELXL-97 package of programs. All non-hydrogen atoms were refined anisotropically. Hydrogen atoms were placed in calculated positions. The final R value was 0.0403 for 1691 observed reflections with $F_0 > 2\sigma(I)$.

CCDC-794469 contains the supplementary crystallographic data for this paper. These data can be obtained free of charge from The Cambridge Crystallographic Data Centre via: www.ccdc.cam.ac.uk/data_request/cif.

[1] W. H. Keeson, *Helium*, Elsevier, Amsterdam, **1942**.
[2] F. E. Simon, C. A. Swenson, *Nature* **1950**, *165*, 829.
[3] J. E. Greedam, *J. Mater. Chem.* **2001**, *11*, 37, and references cited therein.
[4] A. J. Harrison, *J. Phys. Condens. Matter* **2004**, *16*, *S553*, and references cited therein.
[5] P. W. Anderson, *Mater. Res. Bull.* **1973**, *8*, 153.
[6] B. Canals, C. Lacroix, *Phys. Rev. Lett.* **1998**, *80*, *2933*.
[7] L. Balents, *Nature* **2010**, *464*, 199.
[8] P. A. Lee, *Science* **2008**, *321*, *1306*.
[9] A. P. Ramirez, *Nature Phys.* **2008**, *4*, 442.
[10] S. Wessel, M. Olshanii, S. Haas, *Phys. Rev. Lett.* **2001**, *87*, 206407.
[11] I. Mirebeau, I. N. Gonchrenko, P. Cadavez-Peres, S. T. Bramwell, M. J. P. Gingras, J. S. Gardner, *Nature* **2002**, *420*, 54.
[12] I. Mirebeau, I. N. Goncharenko, *J. Phys. Condens. Matter* **2005**, *17*, S771.

[13] J. S. Gardner, S. R. Dunsiger, B. D. Gaulin, M. J. P. Gingras, J. E. Greedam, R. F. Kiefl, M. D. Lumsden, W. A. MacFarlane, N. P. Raju, J. E. Sonier, I. Swainson, Z. Tun, *Phys. Rev. Lett.* **1999**, *82*, 1012.
[14] P. Schiffer, I. Daruka, *Phys. Rev. B* **1997**, *56*, 13712.
[15] X. G. Zheng, H. Kubozono, K. Nisciyama, W. Higemoto, T. Kawae, A. Koda, C. N. Xu, *Phys. Rev. Lett.* **2005**, *95*, 057201.
[16] J. Villain, *J. Phys. C* **1977**, *10*, 1717.
[17] a) B. S. Shastry, B. Sutherland, *Phys. B* **1981**, *108*, 1069; b) S. Chen, H. Buttner, *Eur. Phys. J., B* **2002**, *29*, 15.
[18] R. Moessner, A. P. Ramirez, *Phys. Today* **2006**, *59*, 24.
[19] D. Dai, M.-H. Wangbo, *J. Chem. Phys.* **2004**, *121*, 672.
[20] M. B. Stone, I. A. Zaliznyak, T. Hong, C. L. Broholm, D. H. Reich, *Nature* **2006**, *440*, 187.
[21] R. Taylor, O. Kennard, *J. Am. Chem. Soc.* **1982**, *104*, 5063.
[22] G. R. Desiraju, R. Parthasarthy, *J. Am. Chem. Soc.* **1989**, *111*, 8725.
[23] S. L. Price, A. J. Stone, J. Lucas, R. S. Rowland, A. E. Thornley, *J. Am. Chem. Soc.* **1994**, *116*, 4910.
[24] F. A. Cotton, L. M. Daniels, G. T. Jordan IV, C. A. Murillo, *Chem. Commun.* **1997**, 1673.
[25] R. L. Lintvedt, M. D. Glick, B. K. Tomlonovic, D. P. Gavel, J. M. Kuszaj, *Inorg. Chem.* **1976**, *15*, 1633.
[26] M. Rodriguez, A. Llobet, M. Corbella, *Polyhedron* **2000**, *19*, 2483.
[27] A. Rodriguez-Fortea, P. Alemany, S. Alvarez, E. Ruiz, *Inorg. Chem.* **2002**, *41*, *3769*.
[28] W. E. Hatfield, *Comments Inorg. Chem.* **1981**, *1*,105.
[29] W. E. Hatfield, in: *Magneto-Structural Correlations in Exchange Coupled Systems* (Eds.: R. Willett, D. Gatteschi, O. Kahn), Reidel, Dordrecht, The Netherlands, **1985**.
[30] Carlin, R. L. *Magnetochemistry*, Springer-Verlag, Berlin, **1986**.
[31] G. Van Kalkren, N. N. Schmidt, R. Block, *Phys. Status Solidi B* **1979**, *97*, *315*.
[32] O. Kahn, B. Briat, *J. Chem. Soc. Faraday Trans.* **1976**, *2*, 286.
[33] P. J. Hay, J. C. Thibeault, R. Hoffmann, *J. Am. Chem. Soc.* **1975**, *97*, 4884.
[34] A. Bencini, D. Gatteschi, *Inorg. Chim. Acta* **1978**, *31*, *11*.
[35] W. E. Marsh, K. C. Patel, W. E. Hatfield, D. J. Hodgson, *Inorg. Chem.* **1983**, *22*, 511.
[36] a) O. Kahn, *Molecular Magnetism*, VCH Publishers, New York, **1993**, p. 161; b) O. Kahn, *Molecular Magnetism*, VCH Publishers, New York, **1993**, p. 104.
[37] B. Chiari, O. Piovesana, T. Tarantelli, P. F. Zanazzi, *Inorg. Chem.* **1990**, *29*, 1172.
[38] M. B. Stone, Y. Chen, J. Rittner, H. Yardimci, D. H. Reich, C. Broholm, D. V. Ferraris, T. Lectka, *Phys. Rev. B* **2002**, *65*, 64423.
[39] G. Chaboussant, P. A. Crowell, L. P. Levy, O. Piovesana, A. Madoury, D. Mailly, *Phys. Rev. B* **1997**, *55*, 3046.
[40] P. R. Hammar, D. Reich, *J. Appl. Phys.* **1996**, *79*, 5392.
[41] P. R. Hammar, D. H. Reich, C. Broholm, F. Trouw, *Phys. Rev. B* **1998**, *57*, 7846.
[42] M. Hagiwara, Y. Narumi, K. Kindo, T. Nishido, M. Kamuragi, T. T. Tonegawa, *Phys. B* **1998**, *246–247*, 234.
[43] H. Deguchi, S. Sumoto, S. Takagi, M. Mito, T. Kawae, K. Takeda, H. Nojiri, T. Sakon, M. Motokawa, *J. Phys. Soc. Jpn.* **1998**, *67*, 3707.
[44] R. Calemczuk, J. Riera, D. Poilblanc, J.-P. Boucher, G. Chaboussant, L. P. Levy, O. Piovesana, *Eur. Phys. J., B* **1999**, *7*, 171.
[45] M. Hagiwara, H. A. Katori, U. Schollwock, H.-J. Mikeska, *Phys. Rev. B* **2000**, *62*, 1051.
[46] G. Chaboussant, M.-H. Julien, Y. Fagot-Revurat, L. P. Levy, C. Berthier, M. Horvatic, O. Piovesana, *Phys. Rev. Lett.* **1997**, *79*, 925.
[47] G. Chaboussant, M.-H. Julien, Y. Fagot-Revurat, M. Hanson, L. P. Lévy, C. Berthier, M. Horvatic, O. Piovesana, *Eur. Phys. J., B* **1998**, *6*, 167.
[48] M. Chiba, T. Fukui, Y. Ajiro, M. Hagiwara, T. Goto, T. Kubo, *Phys. B* **1998**, *246–247*, 576.
[49] H. Otha, T. Tanaka, S. Okubo, S. Kimura, H. Kikuchi, H. Nagaosa, *J. Phys. Soc. Jpn.* **1999**, *68*, *732*.
[50] M. Mito, H. Akama, T. Kawae, K. Takeda, H. Deguchi, S. Takagi, *Phys. Rev. B* **2002**, *65*, 104405.
[51] O. A. Starykh, H. Katsura, L. Barents, *Phys. Rev. B* **2010**, *82*, *014421*.
[52] H. Tsujii, C. R. Rotundu, T. Ono, H. Tanaka, B. Andraka, K. Ingersent, Y. Takano, *Phys. Rev. B* **2007**, *76*, 060406.
[53] W. Ashcroft, N. D. Mermin, *Solid State Physics*, Saunders College Publishing, Forth Worth, TX, **1976**.

Received: March 14, 2011
Published Online: August 22, 2011

